ORIGINAL ARTICLE

CrossMark

Imaging the dynamic deposition of cell wall polymer in xylem and phloem in *Populus × euramericana*

Kexia Jin[1] · Xinge Liu[1] · Kun Wang[1] · Zehui Jiang[1] · Genlin Tian[1] · Shumin Yang[1] · Lili Shang[1] · Jianfeng Ma[1]

Abstract

Main conclusion **Both G units and S units deposited in the whole lignification process of xylem fiber.**

The topochemical variations in newly formed xylem and phloem of *Populus × euramericana* were investigated by combined microscopic techniques. During xylem formation, earlier cell wall deposition in vessel and afterwards in the neighboring fiber was observed in situ. Raman images in xylem fiber emphasized that cell wall deposition was an ordered process which lignification started in cell corner following carbohydrates deposition. Higher deposition speed of carbohydrates was revealed at the beginning of the cell wall differentiation, and the syringyl (S) units deposition was more pronounced compared with guaiacyl (G) units at the earlier stage of lignification. The comparative analysis of cell wall composition in phloem fiber indicated that phloem formed earlier than xylem and the distribution of lignin monomers varied significantly with phloem fiber location. Furthermore, an interesting phenomenon was found that the outermost phloem fiber near the periderm displayed a multilayered structure with alternating broad and narrow layer, and the broad lamellae showed higher concentration of carbohydrates and S lignin. The cytological information including cell wall composition and lignin structure of xylem and phloem might be helpful to understand the wood growth progresses and facilitate utilization of woody plants.

Keywords Xylem · Phloem · Cell wall deposition · Lignin monomers · Raman microscopy · *Populus × euramericana*

Introduction

Diameter growth of tree is generated by the activities of the vascular cambium, which can differentiate into secondary xylem in the centripetal direction and phloem in the centrifugal direction. The researches of cambium activity and wood formation have raised considerable attention since they are closely related to tree growth, modification and utilization (Gričar et al. 2015; Lourenço et al. 2016; Nguyen et al. 2017).

The most apparent feature of plant tissue differentiation is formation of cell wall. During cell wall formation, the incorporation of lignin within the polysaccharide cell wall framework is generally regarded as the final stage of the typical differentiating process (Donaldson 2001). Multiple investigations have examined that carbohydrates (cellulose and hemicelluloses) mainly located in the secondary cell wall, and lignin has higher concentration in the cell corner (CC) and compound middle lamella (CML; Ji et al. 2013; Jin et al. 2017; Richter et al. 2011). Lignin is mainly composed of three constitutive monomeric units, namely syringyl (S), guaiacyl (G) and *p*-hydroxyphenyl (H), and its content and composition are extremely variable between species and tissues (Barros et al. 2015; Voxeur et al. 2015). However, previous studies mainly focused on mature wood (secondary xylem), little attention was paid to topochemical changes, especially lignin monomers in various cell types of xylem and phloem during the differentiation process.

In addition, the cell wall structure and composition of the phloem are much less known. Previous researches monitored the dynamic change of phloem formation during growing season, and indicated that phloem formation was less subjected to environmental conditions than the xylem formation (Cufar et al. 2011; Gričar and Čufar 2008; Prislan et al. 2013). Although Lourenço et al. (2016) reported that phloem had a higher lignin content with respect to cork and xylem

✉ Jianfeng Ma
  Majf@icbr.ac.cn

1   Key Lab of Bamboo and Rattan Science & Technology, International Center for Bamboo and Rattan, Beijing 100102, China

tissues, little information was available on cell walls architecture of phloem, and the comparative analysis of cell wall composition and structure in xylem and phloem of the same species was rare.

Investigating the composition and structural components of cell wall has been commonly conducted by optical (Wu et al. 2016; Zhang et al. 2014), electron microscopy (Donaldson and Knox 2012; Rossi et al. 2012) and preparative fractionation (Moniz et al. 2015; Xu et al. 2015) of the plant tissue. However, most traditional analyses of plant cell walls are destructive because they require staining, embedding or disintegration of the plant tissue. Advances in confocal Raman microscopy and imaging have tackled this problem in a noninvasive way to provide chemical and structural information in situ with a high spatial resolution (< 0.5 μm) (Agarwal 2006; Prats et al. 2016; Richter et al. 2011).

The aim of this work is to study the topochemical changes in various cell types of xylem during the differentiation process and comparatively analyze cell wall composition and structure in phloem of the same period by combined microscopic techniques. Such an approach is useful for further investigations on the developmental control of wood formation.

Materials and methods

Materials

Healthy 3-year-old *Populus* (*Populus × euramericana* cv. '74/76') trees with straight boles at breast height were selected within a stand at the Forestry Station in Changping District, Beijing, China (40°17″ N, 116°39″ E). Samples of tissues containing the bark, cambium and the newly formed wood were collected in May 2015. Without any further sample preparation, 5 μm-thick cross-sections were cut from the sample blocks using a sliding microtome (Leica RM2010R, Wetzlar, Germany). For chemical imaging, the samples were placed on a glass slide with a drop of D_2O (Sigma-Aldrich, 99.98 ± 0.01 at.% D), covered by a coverslip (0.17 mm thickness, Thermo Scientific), and sealed with nail polish to prevent evaporation during measurement. Irradiation in D_2O can effectively limit laser-induced fluorescence (Agarwal and Atalla 1986).

Lignin backbone model compounds including G units (coniferyl alcohol, ferulic acid, 2-methoxy-4-methylphenol, 4-hydroxy-3-methoxybenzaldehyde, 3,4-dimethoxytoluene), S units (3,5-dimethoxy-4-hydroxybenzaldehyde, sinapaldehyde, sinapic acid, sinapyl alcohol, 4-methyl-2,6-dimethoxyphenol, 3,4,5-trimethoxytoluene), and carbohydrates model compounds including L-rhamnose, L-fucose, D-galactose, D-glucuronic acid, D-glucose, D-mannose, D-xylose, and L-arabinose were purchased from Sigma-Aldrich (St. Louis, MO).

Methods

Fluorescence and polarized light microscopy

Fluorescence microscopy and light microscope under polarized light with the aid of an image processing and analysis system were used to observe the anatomical features of the xylem and phloem. For fluorescence microscopy (Leica-DM4, Germany), the excitation wavelength was 488 nm and the emission wavelength at 530–600 nm was used. The anatomical observations were carried out on transverse sections.

Raman spectra and Raman mapping

The Raman spectra were acquired with a LabRam Xplora confocal Raman microscope (Horiba Jobin–Yvon, Paris, France). For high spatial resolution, the measurements were conducted with an Olympus high numerical aperture (NA) microscope objective (MPlan 100 × oil, NA = 1.40; Olympus, Tokyo, Japan) and a linear-polarized 532 nm laser. For mapping, 0.3 μm steps were chosen, and every pixel corresponded to one scan. The spectrum from each location was obtained by averaging 2-s cycles. Different chemical images were generated by a cosmic ray removal filter, and default software sum filters (Labspec6, Horiba) were applied to integrate the defined regions in the wood spectra. The filter calculates the intensities within the chosen areas, and the background was subtracted by taking the baseline from the first to the second border. The overview chemical images separated cell wall layers and marked the defined distinct cell wall areas to calculate the average spectra from the areas of interest. Before a detailed analysis, the calculated average spectra were baseline corrected using the linear least squares algorithm.

Results

Heterogeneous deposition pattern of lignin and cellulose at tissue level during cell wall formation

The cambium has been differentiated into xylem and phloem as shown in Fig. 1. The composition of xylem and phloem is visualized by fluorescence and polarized light microscopy, which have been widely applied to explore the lignin and organized cellulose distribution, respectively. In xylem, all the tissues including vessel, xylem ray and fiber are lignified, and in corresponding area the cellulose is distributed evenly. In phloem, lignin mainly locates in periderm, phloem fiber
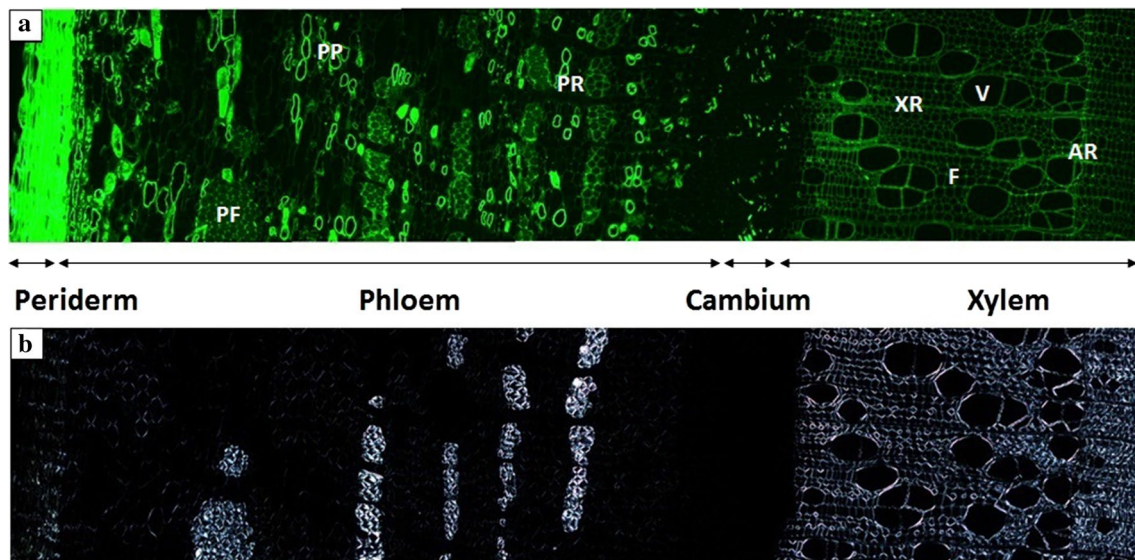
Fig. 1 Anatomy of *Populus* in transverse section by fluorescence microscopy (**a**) and polarized light microscopy (**b**). *PF* phloem fiber, *PP* phloem parenchyma, *PR* phloem ray, *V* vessel, *XR* xylem ray, *F* fiber, *AR* annual ring

and parenchyma, and phloem fiber shows a high birefringence under polarized light (Fig. 1a, b). In this work, components deposition of *Populus* at cellular level was further investigated qualitatively and semi-quantitatively by Raman microspectroscopic imaging approach.

Heterogeneous deposition pattern of lignin and carbohydrates at cellular level during cell wall formation

Raman band assignments of model compounds and *Populus* samples

The plant cell wall is mainly composed of cellulose, hemicelluloses, and lignin. In *Populus* (hardwood), lignin is primarily composed of guaiacyl (G) and syringyl (S) units (Agarwal 2006). To determine spectral fingerprints for the characteristic bands of G and S units, spectra of lignin backbone model compounds representing a specific structure were grouped together and the repeating Raman bands were identified (Fig. 2a, b). Since G and S units share some common molecular structures, there are two overlapping Raman band regions (1583–1617 and 1445–1267 cm^{-1}) associated with these units, and thus they are not used for assignments of lignin units in current work. By comparing the unique ring structures derived from several model compounds, multiple nonoverlapping band ranges can be determined for them individually: 1166–1197, 1255–1290 cm^{-1} for G units, and 1320–1338 cm^{-1} for S units. The bands range from 1166 to 1197 cm^{-1} also overlap with *p*-hydroxyphenyl units of lignin (Sun et al. 2012) and not present in the spectra of *Populus* samples (Fig. 2d). Considering above factors, it is

appropriately identified 1255–1290 cm^{-1} for G units and 1320–1338 cm^{-1} for S units. The two Raman bands of G and S units are verified at 1272 and 1333 cm^{-1} in *Populus* samples, where the G units is assigned to aromatic ethers stretch, and S units is attributed to aryl-O–CH$_3$ vibration, respectively (Saariaho et al. 2003). This is further supported by the work of Agarwal et al. (2011) which based on FT-Raman investigation of hardwood and softwood milled-wood lignins, it was reported that the Raman intensity of lignin band at 1331 cm^{-1} was stronger in the hardwood compared with the softwood, and the opposite was true for the band at 1272 cm^{-1}. The other lignin features in *Populus* samples are detected at 1600, 1656 and 2935 cm^{-1} (Fig. 2d). Strong band at 2935 cm^{-1} from the C–H stretch of the methoxyl groups of the lignin. The peak around 1600 cm^{-1} points to the stretching vibrations of the aromatic ring and that at 1656 cm^{-1} to ring-conjugated C=C bonds in coniferyl alcohol units (Agarwal 2006; Larsen and Barsberg 2010).

Meanwhile, the Raman bands of model compounds of cellulose (D-glucose) and hemicelluloses (D-arabinose, D-xylose, D-mannose, D-glucuronic acid, D-galactose, L-fucose, and L-rhamnose) were investigated (Fig. 2c). Cellulose model has obvious shoulders around 1074, 1120, 1344, 1460, 2890, and 2940 cm^{-1}. It is noted that some of peaks overlap with characteristic bands of hemicelluloses (1120, 2890, and 2937 cm^{-1}) and lignin (1460, 2935 cm^{-1}). Besides, there is some Raman shift existing between model compounds and *Populus* sample for the lignin covalent bond in plant cell wall, thus the corresponding bands of carbohydrates (cellulose and hemicelluloses) are observed at 1097, 1125, 1379 and 2889 cm^{-1} in *Populus* (Fig. 2d). The peaks at 1097 and 1125 cm^{-1} are attributed to asymmetric and
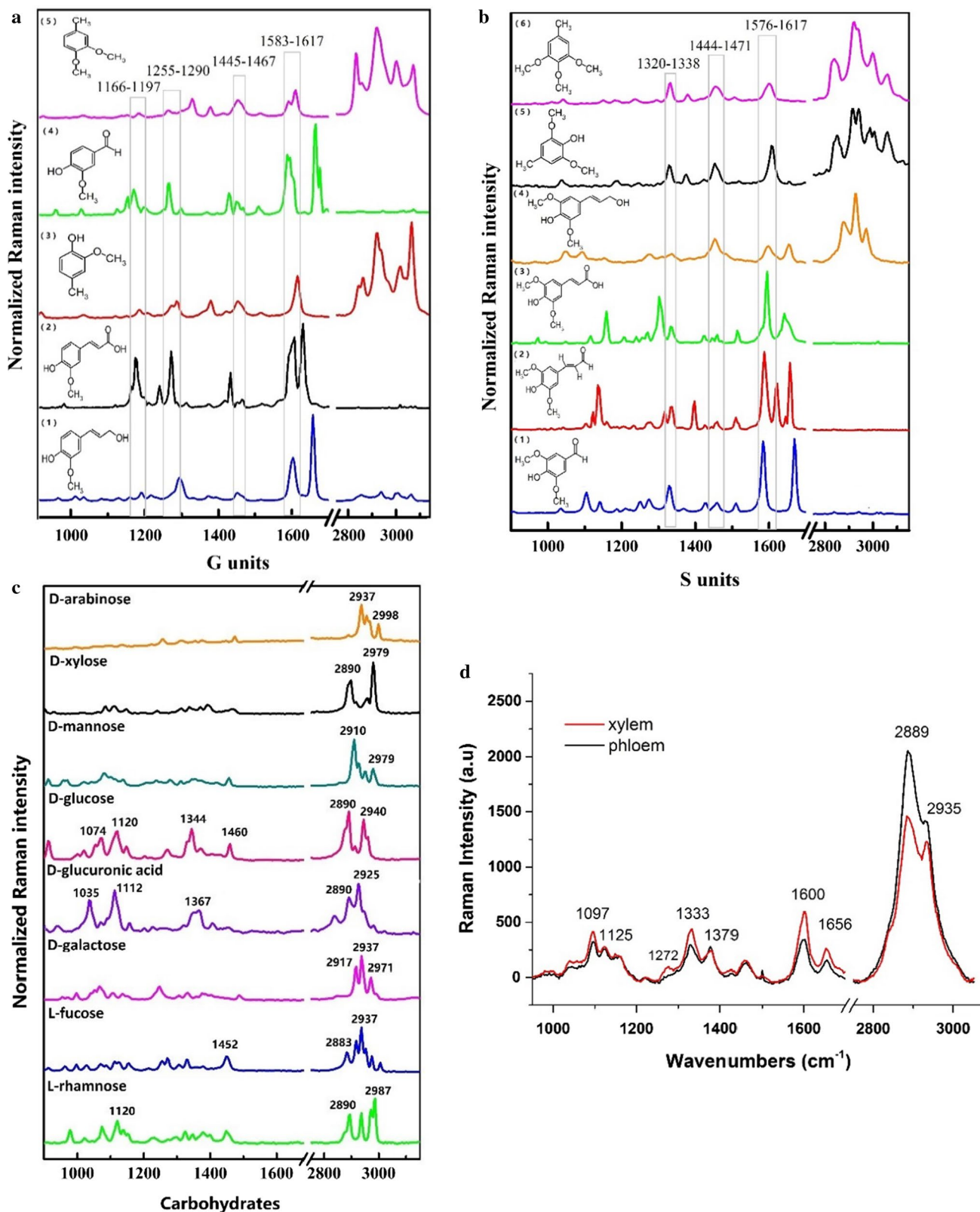
Fig. 2 FT-Raman spectra of model compounds [**a** G units: (1) coniferyl alcohol, (2) ferulic acid, (3) 2-methoxy-4-methylphenol, (4) 4-hydroxy-3-methoxybenzaldehyde and (5) 3,4-dimethoxytoluene, **b** S units: (1) 3,5-dimethoxy-4-hydroxybenzaldehyde, (2) sinapaldehyde, (3) sinapic acid, (4) sinapyl alcohol, (5) 4-methyl-2,6-dimeth-oxyphenol and (6) 3,4,5-trimethoxytoluene, **c** carbohydrates: including L-rhamnose, L-fucose, D-galactose, D-glucuronic acid, D-glucose, D-mannose, D-xylose, and L-arabinose] and *Populus* xylem and phloem (**d**)

symmetric stretch of C–O–C linkages, respectively. A band at 1379 cm^{-1} is assigned to HCC, HCO, and HOC bending, and the shoulder at 2889 cm^{-1} represents stretching of C–H and C–H$_2$ groups (Agarwal and Ralph 1997; Agarwal et al. 2011; Kanbayashi and Miyafuji 2015; Wiley and Atalla 1987).

Changes in cell wall composition of the xylem and phloem

For an overview of the measurement areas, Raman image with all cell wall structures of xylem were calculated by integrating over the CH-stretching region (2800–3030 cm^{-1}), in which all cell walls polymers (carbohydrates and lignin) contributed to the Raman signal (Fig. 3a, b). Near the cambium, where the newly formed xylem has been differentiated into various cell types, higher carbohydrates concentration is observed in the outer layer of secondary wall (SW) by integrating from 2800 to 2918 cm^{-1} (Fig. 3c). Lignin distribution is also visualized by calculating the band ranges from 1540 to 1700 cm^{-1} (Fig. 3e). Vessel and ray parenchyma have higher amounts of lignin at earlier stage of lignification. In fiber, in contrast, slight lignin is mainly deposited in CC. By integrating from the region of 1255–1290 cm^{-1} (G units) and 1320–1338 cm^{-1} (S units), respectively, it is found that the concentration of S units is more pronounced than G units in corresponding region (Fig. 3g, i). With secondary thickening, high intensity and, therefore, high carbohydrates concentration is visualized in fiber, followed by vessel and the fewest in ray parenchyma. At sub-cellular level, carbohydrates concentration in SW is higher than that in CC and CML, and lignin concentration in morphological region exhibits an opposite trend (Fig. 3d, f). More S units deposition occurs in vessel, ray parenchyma, and fiber at later stage of lignification, while G units is mainly deposited in CC of fiber and vessel wall (Fig. 3h, j).

To further explore the variation of cell wall composition in newly formed xylem fiber, the Raman spectra attributed to carbohydrates (1097, 1125, 1379 and 2889 cm^{-1}) and lignin (1272, 1333, 1600 and 1656 cm^{-1}) in SW and CC of 10 cells near the cambium (Nos. 1–10 in Fig. 3a) and 5 cells near the annual ring (Nos. 11–15 in Fig. 3b) were extracted, respectively (Fig. 4). Higher deposition speed of carbohydrates is revealed at earlier stage (the cells Nos. 1–7) both in SW and CC, which the Raman intensity of the main carbohydrates signature (2889 cm^{-1}) quickly exceeds 1100 cts. At later stage (the cells Nos. 8–15), the carbohydrates deposition shows a slower growth trend, which the increase of Raman band at 2889 cm^{-1} is within 500 cts, and other carbohydrates signature peaks are less than 200 cts (Fig. 4a, b). The significant increase of Raman intensity for lignin bands are observed at the No. 3 cell in CC, and in SW after the No. 7 cell. Meanwhile, CC shows much higher Raman intensity than SW (Fig. 4c, d). When the Raman intensity of main lignin signature peak (1600 cm^{-1}) reaches 3000 cts in CC, the corresponding Raman intensity in SW is lower than 800 cts, and the other lignin bands in CC are at least 2.5 times higher than in SW during secondary thickening process.

In contrast to immature xylem fiber, the phloem fiber near the cambium has finished secondary thickening. In mature phloem fiber, carbohydrates are mainly distributed in SW, and lignin is mainly located in CC and CML (Fig. 5d–i). However, the distribution and concentration of lignin monomers in CC and CML region vary significantly with phloem fiber location. The concentration of G units is more pronounced than S units both in CC and CML of the innermost phloem fiber which near the cambium, and the phloem fiber in the middle region displays an opposite trend (Fig. 5k, l, n, o). In the outermost of phloem which near the periderm, the phloem fiber has higher concentration of G units in CC area, while in CML the Raman intensity of S units is more evident
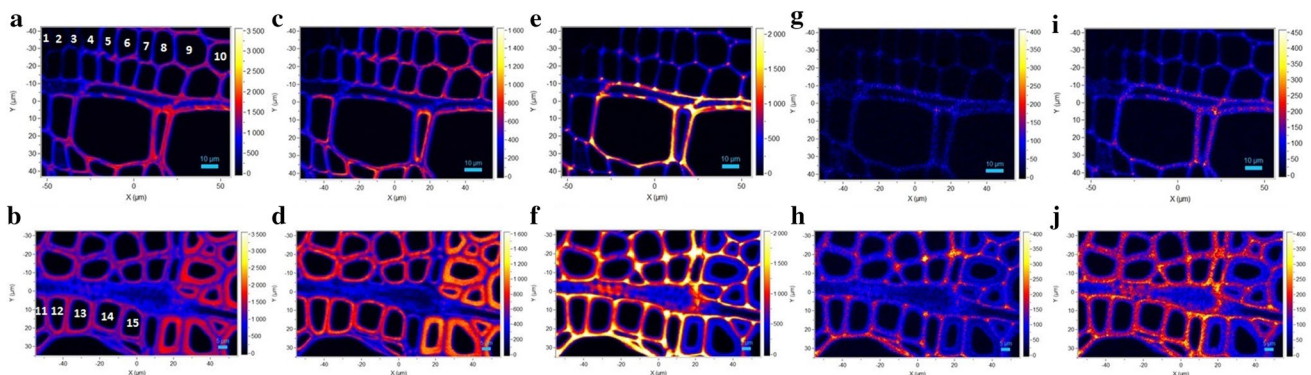

Fig. 3 Raman images of xylem for *Populus* calculated by integrating from 2800 to 3030 cm^{-1} (**a**, **b** overall morphology), from 2800 to 2918 cm^{-1} (**c**, **d** carbohydrates), from 1540 to 1700 cm^{-1} (**e**, **f**, lignin), from 1255 to 1290 cm^{-1} (**g**, **h** G units), and from 1320 to 1338 cm^{-1} (**i**, **j**, S units). Images **a**, **c**, **e**, **g**, **i**: xylem near the cambium and images **b**, **d**, **f**, **h**, **j** xylem near the annual ring (AR)
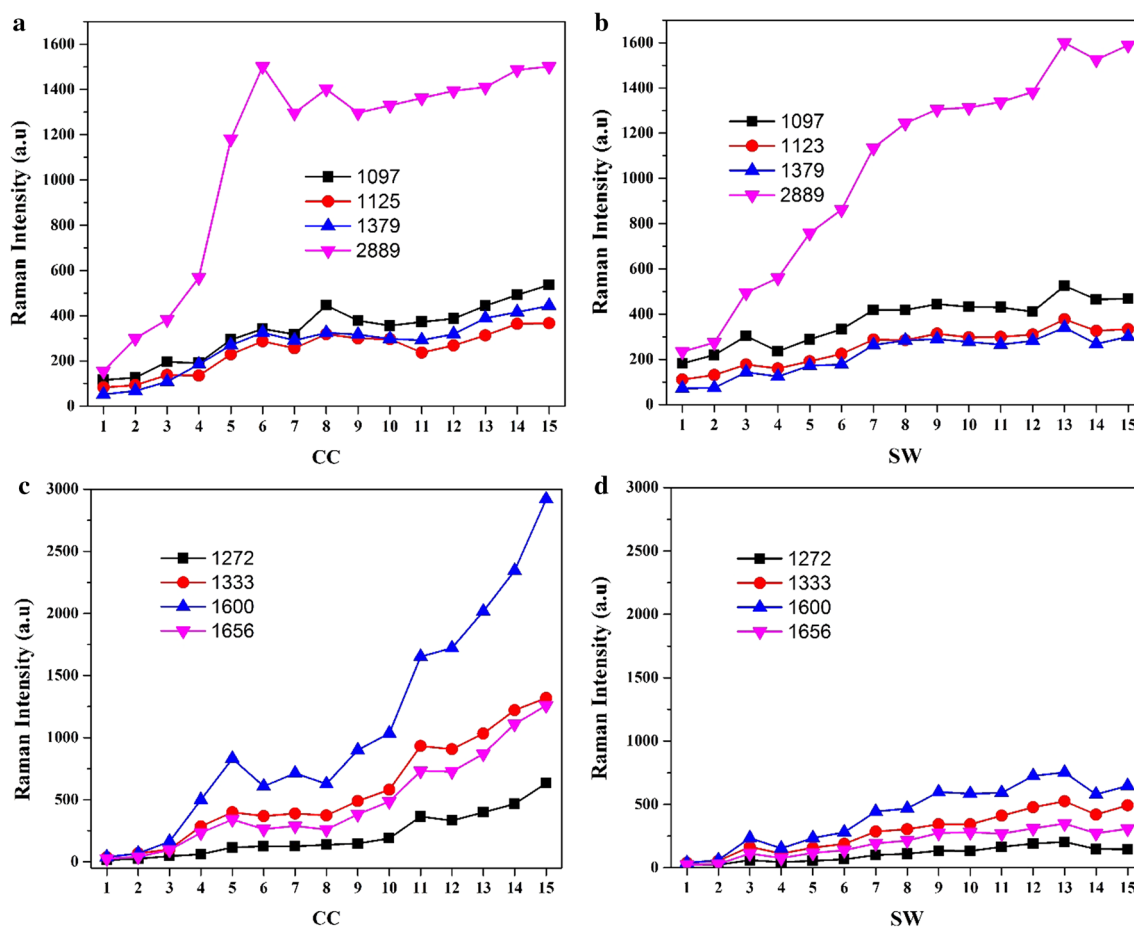
Fig. 4 The Raman intensity of carbohydrates (**a**, **b**) and lignin (**c**, **d**) in CC and SW of the fibers. Nos. 1–10 on the *x*-axis are the fibers near the cambium, and Nos. 11–15 are the fibers near the annual ring

(Fig. 5j, m). From the overall morphology of phloem fiber by integrating from 2800 to 3030 cm^{-1}, an interesting phenomenon is found that the outermost phloem fiber evolves into a multilayered structure with alternating broad and narrow lamellae (Fig. 5a). The bands at 1333, 1600, and 2889 cm^{-1} show higher intensity within broad lamellae compared to the narrow lamellae (Fig. 6), indicating broad lamellae have higher concentration of carbohydrates and S lignin.

Discussion

Vessel and fiber are the major tissues of xylem (Ma et al. 2011; Jin et al. 2017). Earlier cell wall deposition in vessel and afterwards in the neighboring fiber was observed. Meanwhile, G units showed higher concentration in vessel than in fiber cells. Similar temporal delay in SW thickening and lignification between vessel and neighboring tissues has also been observed in other species (Marion et al. 2007; Prislan et al. 2009). Vessel has an important function for water and nutrient transportation during wood formation (Payvandi

et al. 2014). The cell wall deposition completed in advance in vessel could transport water and nutrient to adjacent cells and contribute to cells development. A more rapid lignin deposition in vessel would lead to more G units structure formed (Lourenço et al. 2016). This explains why vessel lignify earlier than fiber and contains high concentration of G units, while fiber shows less G and more S units.

In fiber cells, when carbohydrates distributed evenly in SW, the lignin was highlighted in the CC area, and in SW the lignin concentration was much lower, indicating the cell wall deposition is an ordered developmental process. Higher deposition speed of carbohydrates at earlier stage of cell wall differentiation was revealed by extracting the Raman spectra of fiber. Carbohydrates as the main composition of cell wall deposited first with a higher speed, then lignin filled the voids between carbohydrates to create a rigid and compact structure of plant cell wall (Zhao et al. 2012). Lignification started in the CC with a mixture of G and S units, then more G units was deposited in CC region and S units in CML, and finally the incorporation of G and S units spread into SW following carbohydrates deposition, thus resulted
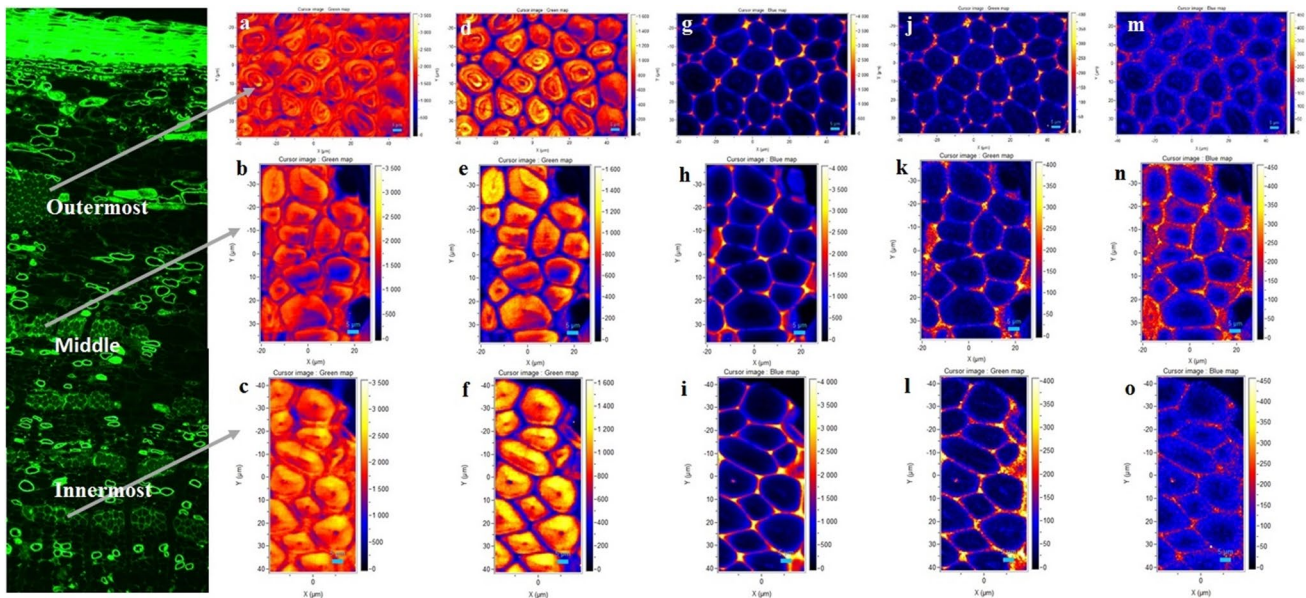
Fig. 5 Raman images of phloem fibers for *Populus* calculated by integrating from 2800 to 3030 cm^{-1} (**a–c** overall morphology), from 2800 to 2918 cm^{-1} (**d–f** carbohydrates), from 1540 to 1700 cm^{-1} (**g–i** lignin), from 1255 to 1290 cm^{-1} (**j–l** G units), and from 1320 to 1338 cm^{-1} (**m–o** S units). Images **a**, **d**, **g**, **j**, **m** the outermost phloem fiber near the periderm, images **b**, **e**, **h**, **k**, **n** phloem fiber in the middle of phloem, and images **c**, **f**, **i**, **l**, **o** the innermost phloem fiber near the cambium
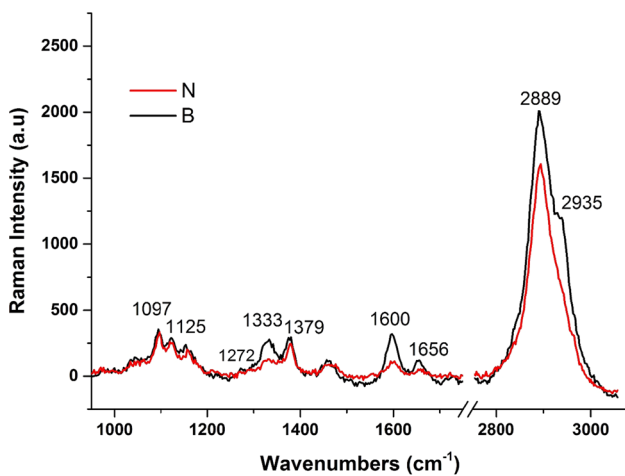

Fig. 6 The Raman spectra of broad (B) and narrow (N) lamellae in outermost of the phloem fiber

in more lignin accumulation in CC as compared with in SW (Fig. 3e–j). The lignification of the SW commenced after the CML lignin concentration reached approximately 50% of its maximum, and the main lignification became active after plant SW thickening was complete (Donaldson 2001; Terashima and Fukushima 1988). Although previous literatures showed that the deposition of G units continues throughout the early to late stages, and S units are deposited mainly during the later stage (Donaldson 2001; Fukushima and Terashima 1991; Rencoret et al. 2011), the results from

Raman spectra and images indicated that deposition of S units also is pronounced at the earlier stage of cell differentiation compared with G units. This is consistent with the investigation of Rencoret et al. (2011) that both young and adult *Eucalyptus globulus* had higher content of S units than G units.

Although it has been well-established that lignification appears after carbohydrates deposition (Boerjan et al. 2003; Donaldson 2001; Donaldson and Knox 2012), the research of dynamic deposition of cell wall polymer during xylem formation was limited. By extracting the Raman spectra of fiber, the intensity of carbohydrates and lignin related Raman bands showed a continuously increasing trend with the increase of the distance from the cambium, indicating carbohydrates and lignin deposited constantly during xylem formation. Nevertheless, small decrease or sharp increase of Raman intensity in individual cell was observed. This fact suggested the differentiation of cell wall is a dynamic and plastic process which is highly associated with weather conditions (Rowe and Speck 2005). Lower seasonal temperature could shorten regular cambial activity and slow down cell wall deposition, and higher precipitation may promote cell wall production thus affect cell wall differentiation (Gričar et al. 2007, 2015).

In phloem fiber, investigating topochemical variation in cell wall composition was rare in the last two decades (Cufar et al. 2011; Gričar and Čufar 2008), and the information regarding monomeric composition were inconsistent from the limited literatures. Christiernin (2006) demonstrated that

phloem cells had more G units comparatively to wood cells in *Populus*. Conversely, Lourenço et al. (2016) supported that S units were presented more from phloem in *Quercus suber*. According to our observations, the relative concentration and distribution of lignin monomers varied with cell location. For instance, the phloem fiber near the cambium has higher concentration of G units, whereas phloem fiber in the middle region shows an opposite trend. Therefore, the cell wall composition in phloem needs further investigation, maybe this completely opposite results not only arise from variation in species, also depend on the location of the sample.

On the other hand, the structure of phloem fiber also changed with cell location. Unlike the regular sclerenchyma cell of phloem fiber in the innermost and middle part of phloem, the outermost phloem fiber near the periderm showed a multilayered structure with alternating broad and narrow lamellae (Fig. 5c). This concentric layered structure was first time reported in *Populus*, to the best of our knowledge. Similar structure was observed in bamboo and rattan (Liu et al. 2017; Lybeer and Koch 2005; Parameswaran and Liese 1976). This lamellation consists of alternating broad and narrow layers with differing chemical composition, which leads to an extremely high tensile strength, as demonstrated in engineering constructions with bamboo culms (Parameswaran and Liese 1977). Nevertheless, on the contrary to the result from bamboo and rattan, the broad lamellae in *Populus* have higher concentration of both carbohydrates and lignin. In this respect, the mechanical properties of *Populus* phloem and comparing with other wood need further investigation in future studies.

When comparing the cell wall formation between xylem and phloem by cambium activity, semi-quantitative results indicated that the Raman intensity of xylem cell wall composition was lower than phloem cell during the same period, and suggested that the formation of phloem occurred before xylem. Similar observations were found for the same species that grown in same latitude by Xi and Zhao (2013). Earlier study reported that phloem of *Populus* differentiated about 3 weeks earlier than xylem formation, and xylem differentiation began in late April (Yin et al. 2002). Opposite order or same time with phloem and xylem differentiation by cambium activity also appeared in other species (Akm and Hashmi 1983; Cui et al. 1995). Gričar et al. (2014) investigated *Picea abies* trees from three contrasting sites, differing in altitude and latitude, and found in all cases the cambium simultaneously started and stopped producing xylem and phloem cells. In consequence, it is reasonable to assume that different division pattern of cambium is related with tree species.

The cytological information including cell wall composition and lignin structure can be obtained in situ by confocal Raman microscopy. Since the chemical constitution of cell wall is closely related to its application, such as fermentable sugar release in biofuel production, delignification in pulping technology, and conversion into high value co-products (Delgado et al. 2016; Korhonen et al. 2011; Pinto et al. 2015; Zeng et al. 2014), the information of cell wall architecture and composition from tissue level to the cellular level might be helpful in understanding wood growth and facilitate wood utilization.

Conclusion

Combined microscopic techniques have been used to nondestructively investigate the structural diversity and compositional heterogeneity in *Populus* at multi-scale. The Raman bands of carbohydrates and lignin (G and S units) were verified in *Populus* samples by comparing a series of model compounds. Extracting the Raman spectra attributed to carbohydrates and lignin, higher speed of carbohydrates deposition was revealed at the beginning of the cell wall differentiation. Lignin distribution near the cambium and annual ring in xylem indicated not only G units deposited throughout the early to late stages, but also S units deposition involved in the whole lignification process in xylem fiber. In phloem fiber, the distribution and concentration of lignin monomers varied significantly with location, which G units were predominant in the innermost and outermost fiber, whereas S units were present in much higher amounts in the middle region. Furthermore, a multilayered structure with alternating broad and narrow layer was found for the first time in phloem fiber near the periderm, and the broad lamellae had higher concentration of carbohydrates and S lignin.

References

Agarwal UP (2006) Raman imaging to investigate ultrastructure and composition of plant cell walls: distribution of lignin and cellulose

in black spruce wood (*Picea mariana*). Planta 224(5):1141–1153. https://doi.org/10.1007/s00425-006-0295-z

Agarwal UP, Atalla RH (1986) In situ Raman microprobe studies of plant cell walls: macromolecular organization and compositional variability in the secondary wall of *Picea mariana* (Mill.) B.S.P. Planta 169(3):325–332. https://doi.org/10.1007/b00392127

Agarwal UP, Ralph SA (1997) FT-Raman spectroscopy of wood: identifying contributions of lignin and carbohydrate polymers in the spectrum of black spruce (*Picea mariana*). Appl Spectrosc 51(11):1648–1655. https://doi.org/10.1016/j.agrformet.2013.06.001

Agarwal UP, McSweeny JD, Ralph SA (2011) FT-Raman investigation of milled wood lignins: softwood, hardwood, and chemically modified black spruce lignins. J Wood Chem Technol 31(4):324–344. https://doi.org/10.1080/02773813.2011.562338

Akm G, Hashmi S (1983) Periodicity of cambium and the formation of xylem and phloem in *Mimusops elengi* L., an evergreen member of tropical India. Flora Morphol Geobot Oekophysiol 197:479–487

Barros J, Serk H, Granlund I et al (2015) The cell biology of lignification in higher plants. Ann Bot 115(7):1053–1074. https://doi.org/10.1093/aob/mcv046

Boerjan W, Ralph J, Baucher M (2003) Lignin biosynthesis. Annu Rev Plant Biol 54(1):519–546. https://doi.org/10.1146/annurev.arplant.54.031902.134938

Christiernin M (2006) Lignin composition in cambial tissues of poplar. Physiol Biochem 44:700–706. https://doi.org/10.1016/j.plaphy.2006.10.012

Čufar K, Cherubini M, Gričar J et al (2011) Xylem and phloem formation in chestnut (*Castanea sativa* Mill.) during the 2008 growing season. Dendrochronologia 29(3):127–134. https://doi.org/10.1016/j.dendro.2011.01.006

Cui KM, Wei LB, Li JH et al (1995) Periodicity of cambial activity and changes of starch content in *Broussonetia papyrifera*. Acta Bot Sin 37(1):53–57

Delgado AM, González I, Tarrés Q et al (2016) The key role of lignin in the production of low-cost lignocellulosic nanofibres for papermaking applications. Ind Crops Prod 86:295–300. https://doi.org/10.1016/j.indcrop.2016.04.010

Donaldson LA (2001) Lignification and lignin topochemistry—an ultrastructural view. Phytochemistry 57(6):859–873. https://doi.org/10.1016/s0031-9422(01)00049-8

Donaldson LA, Knox JP (2012) Localization of cell wall polysaccharides in normal and compression wood of radiata pine: relationships with lignification and microfibril orientation. Am Soc Plant Biol 158(2):642–653. https://doi.org/10.1104/pp.111.184036

Fukushima K, Terashima N (1991) Heterogeneity in formation of lignin. XIV. Formation and structure of lignin in differentiating xylem of *Ginkgo biloba*. Holzforschung 45:87–94. https://doi.org/10.1515/hfsg.1991.45.2.87

Gričar J, Čufar K (2008) Seasonal dynamics of phloem and xylem formation in silver fir and Norway spruce as affected by drought. Russ J Plant Physiol 55(4):538–543. https://doi.org/10.1134/s1021443708040016x

Gričar J, Zupančič M, Čufar K et al (2007) Regular cambial activity and xylem and phloem formation in locally heated and cooled stem portions of Norway spruce. Wood Sci Technol 41(6):463–475. https://doi.org/10.1007/s00226-006-0109-2

Gričar J, Prislan P, Gryc V et al (2014) Plastic and locally adapted phenology in cambial seasonality and production of xylem and phloem cells in *Picea abies* from temperate environments. Tree Physiol 34(8):869–881. https://doi.org/10.1093/treephys/tpu026

Gričar J, Prislan P, De LM et al (2015) Plasticity in variation of xylem and phloem cell characteristics of Norway spruce under different local conditions. Front Plant Sci 6:730–743. https://doi.org/10.3389/fpls.2015.00730

Ji Z, Ma JF, Zhang ZH et al (2013) Distribution of lignin and cellulose in compression wood tracheids of *Pinus yunnanensis* determined by fluorescence microscopy and confocal Raman microscopy. Ind Crops Prod 47(3):212–217. https://doi.org/10.1016/j.indcrop.2013.03.006

Jin KX, Cui HS, Liu XE et al (2017) Topochemical correlation between carbohydrates and lignin on *Eucommia ulmoides* cell wall from tissue to cell level. BioResources 12(1):1064–1076. https://doi.org/10.15376/biores.12.1.1064-1076

Kanbayashi T, Miyafuji H (2015) Raman microscopic analysis of wood after treatment with the ionic liquid, 1-ethyl-3-methylimidazolium chloride. Holzforschung 69(3):273–279. https://doi.org/10.1515/hf-2014-0060

Korhonen JT, Kettunen M, Ras RH et al (2011) Hydrophobic nanocellulose aerogels as floating, sustainable, reusable, and recyclable oil absorbents. ACS Appl Mater Interfaces 3(6):1813–1816. https://doi.org/10.1021/am200475b

Larsen KL, Barsberg S (2010) Theoretical and Raman spectroscopic studies of phenolic lignin model monomers. J Phys Chem B 114(23):8009–8021. https://doi.org/10.1021/jp1028239

Liu XE, Jin KX, Cui HS, Ma JF (2017) The lignin topochemistry of *Daemonorops margaritae* (Hance) Becc. molecular spectroscopic imagine. Spectrosc Spectr Anal 37(17):3138–3144

Lourenço A, Rencoret J, Chemetova C et al (2016) Lignin composition and structure differs between xylem, phloem and phellem in *Quercus suber* L. Front Plant Sci 7:1612–1626. https://doi.org/10.3389/fpls.2016.01612

Lybeer B, Koch G (2005) A topochemical and semiquantitative study of the lignification during ageing of bamboo culms (*Phyllostachys viridiglaucescens*). IAWA J 26(1):99–109. https://doi.org/10.1163/22941932-90001605

Ma JF, Yang GH, Mao JZ et al (2011) Characterization of anatomy, ultrastructure and lignin microdistribution in *Forsythia suspensa*. Ind Crops Prod 33(2):358–363. https://doi.org/10.1016/j.indcrop.2010.11.009

Marion L, Gričar J, Oven P (2007) Wood formation in urban Norway maple trees studied by the micro-coring method. Dendrochronologia 25(2):97–102. https://doi.org/10.1016/j.dendro.2007.05.001

Moniz P, Lino J, Duarte LC et al (2015) Fractionation of hemicelluloses and lignin from rice straw by combining autohydrolysis and optimized mild organosolv delignification. BioResources 10(2):2626–2641. https://doi.org/10.15376/biores.10.2.2626-2641

Nguyen VP, Cho JS, Lee JH et al (2017) Identification and functional analysis of a promoter sequence for phloem tissue specific gene expression from *Populus trichocarpa*. J Plant Biol 60(2):129–136. https://doi.org/10.1007/s12374-016-0904-8

Parameswaran N, Liese W (1976) On the fine structure of bamboo. Wood Sci Technol 10(4):231–246. https://doi.org/10.1007/bf00350830

Parameswaran N, Liese W (1977) Structure of septate fibers in bamboo. Holzforschung 31(2):55–57. https://doi.org/10.1515/hfsg.1977.31.2.55

Payvandi S, Daly KR, Jones DL et al (2014) A mathematical model of water and nutrient transport in xylem vessels of a wheat plant. Bull Math Biol 76(3):566–596. https://doi.org/10.1007/s11538-013-9932-4

Pinto PCR, Oliveira C, Costa CA et al (2015) Kraft delignification of energy crops in view of pulp production and lignin valorization. Ind Crops Prod 71:153–162. https://doi.org/10.1016/j.indcrop.2015.03.069

Prats MB, Hauser MT, Heredia A et al (2016) Waterproofing in *Arabidopsis*: following phenolics and lipids in situ by confocal Raman microscopy. Front Chem 4:10–22. https://doi.org/10.3389/fchem.2016.00010

Prislan P, Koch G, Čufar K et al (2009) Topochemical investigations of cell walls in developing xylem of beech (*Fagus sylvatica*

L.). Holzforschung 63(4):482–490. https://doi.org/10.1515/hf.2009.079

Prislan P, Gričar J, Luis MD et al (2013) Phenological variation in xylem and phloem formation in *Fagus sylvatica*, from two contrasting sites. Agric For Meteorol 180(8):142–151. https://doi.org/10.1016/j.agrformet.2013.06.001

Rencoret J, Gutiérrez A, Nieto L et al (2011) Lignin composition and structure in young versus adult *Eucalyptus globulus* plants. Plant Physiol 155:667–682. https://doi.org/10.1104/pp.110.167254

Richter S, Müssig G, Gierlinger N (2011) Functional plant cell wall design revealed by the Raman imaging approach. Planta 233(4):763–772. https://doi.org/10.1007/s00425-010-1338-z

Rossi S, Morin H, Deslauriers A (2012) Causes and correlations in cambium phenology: towards an integrated framework of xylogenesis. J Exp Bot 63(5):2117–2126. https://doi.org/10.1093/jxb/err423

Rowe N, Speck T (2005) Plant growth forms: an ecological and evolutionary perspective. N Phytol 166(1):61. https://doi.org/10.1111/j.1469-8137.2004.01309.x

Saariaho AM, Jääskeläinen AS, Nuopponen M et al (2003) Ultra violet resonance Raman spectroscopy in lignin analysis: determination of characteristic vibrations of *p*-hydroxyphenyl, guaiacyl, and syringyl lignin structures. Appl Spectrosc 57(1):58–66. https://doi.org/10.1366/000370203321165214

Sun L, Varanasi P, Yang F et al (2012) Rapid determination of syringyl: guaiacyl ratios using FT-Raman spectroscopy. Biotechnol Bioeng 109(3):647–656. https://doi.org/10.1002/bit.24348

Terashima N, Fukushima K (1988) Heterogeneity in formation of lignin—XI: an autoradiographic study of the heterogeneous formation and structure of pine lignin. Wood Sci Technol 22(3):259–270. https://doi.org/10.1007/bf00386021

Voxeur A, Wang Y, Sibout R (2015) Lignification: different mechanisms for a versatile polymer. Curr Opin Plant Biol 23:83–90. https://doi.org/10.1016/j.pbi.2014.11.006

Wiley JH, Atalla RH (1987) Band assignments in the Raman spectra of celluloses. Carbohydr Res 160(87):113–129. https://doi.org/10.1016/0008-6215(87)80306-3

Wu H, Xu H, Li H et al (2016) Seasonal development of cambial activity in relation to xylem formation in Chinese fir. J Plant Physiol 195:23–30. https://doi.org/10.1016/j.jplph.2015.12.013

Xi EH, Zhao GJ (2013) Seasonal development of cambium and secondary xylem in *Populus × euramericana ck*. '74/76' during the 2010 growing season. Wood Res 58(3):425–438

Xu JK, Sun YC, Sun RC (2015) Synergistic effects of ionic liquid plus alkaline pretreatments on eucalyptus: lignin structure and cellulose hydrolysis. Process Biochem 50(6):955–965. https://doi.org/10.1016/j.procbio.2015.03.014

Yin YF, Jiang XM, Wei LB (2002) Periodicity of cambium activity and changes of peroxidase isozymes in *Populus tomentosa* Carr. Sci Silvae Sin 38(1):103–110

Zeng YN, Zhao S, Yang S, Ding SY (2014) Lignin plays a negative role in the biochemical process for producing lignocellulosic biofuels. Curr Opin Biotechnol 27(6):38–45. https://doi.org/10.1016/j.copbio.2013.09.008

Zhang J, Nieminen K, Serra JA et al (2014) The formation of wood and its control. Curr Opin Plant Biol 17(1):56–63. https://doi.org/10.1016/j.pbi.2013.11.003

Zhao X, Zhang L, Liu D et al (2012) Biomass recalcitrance. Part I: the chemical compositions and physical structures affecting the enzymatic hydrolysis of lignocellulose. Biofuels Bioprod Biorefin 6(4):465–482. https://doi.org/10.1002/bbb.1331